applied sciences

MDPI

Article

Baseline Particulate Matter Characteristics and Microbial Composition in Air Samples from Natural and Urban Environments: A First Combined Genomic and Microscopy Analysis

János Pálhalmi [1,*], Marcin Niemcewicz [2], Łukasz Krzowski [3], Anna Mező [1], Rafał Szelenberger [2], Marcin Podogrocki [2] and Michal Bijak [2,*]

[1] DataSenseLabs Ltd., Király u. 80., Fsz. 11., 1068 Budapest, Hungary; anna.mezo@datasenselabs.net
[2] Biohazard Prevention Centre, Faculty of Biology and Environmental Protection, University of Lodz, Pomorska 141/143, 90-236 Lodz, Poland; marcin.niemcewicz@biol.uni.lodz.pl (M.N.); rafal.szelenberger@biol.uni.lodz.pl (R.S.); marcin.podogrocki@biol.uni.lodz.pl (M.P.)
[3] Biodefense Laboratory, Biomedical Engineering Centre, Institute of Optoelectronics, Military University of Technology, gen. Sylwestra Kaliskiego 2, 00-908 Warsaw, Poland; lukasz.krzowski@wat.edu.pl
* Correspondence: janos.palhalmi@datasenselabs.net (J.P.); michal.bijak@biol.uni.lodz.pl (M.B.)

Featured Application: The rapid detection and identification of biological agents, crucial for medical diagnostics, environmental monitoring, and biodefense, remains a significant challenge. Combining microscopic analysis with genetic studies enables the identification of biomass, and when paired with the growing field of deep machine learning, these methods could swiftly detect changes in particulate matter and microbial composition, particularly in the context of chemical, biological, radiological, and nuclear (CBRN) threats. Conducting such analyses on a large scale holds significant potential for creating a unique database, enabling the comparison of airborne biomass and accelerating the detection of anomalies, such as the intentional or unintentional release of bacteria into the environment.

Abstract: This study examines the differences in particulate matter (PM) properties and microbial compositions between natural and urban environments, providing foundational data for environmental monitoring and biothreat detection. Air samples were collected during the spring and early summer from two distinct locations: a forest/lake area, and an urban parking lot adjacent to a high-traffic roadway. Quantitative phase imaging microscopy and genomic sequencing were employed to characterize particle size distributions, statistical properties, and microbial community structures in these environments. The results revealed significant differences in PM properties between the two locations. Urban air exhibited higher particle concentrations that reflect pollution sources, whereas the natural environment displayed greater variability in particle size and distribution, correlating with diverse biological content. Genomic sequencing showed a lower diversity of microbial communities compared to the forest/lake area but with greater uniformity. To sum up, by integrating optical microscopy and genomic sequencing, this research demonstrates the feasibility of establishing environmental baselines for PM characteristics and bio-component diversity. The findings underscore the potential of combining real-time optical sensing with genomic tools for early biothreat detection and improved environmental monitoring in diverse settings.

Keywords: microscopy; genomic sequencing; particulate matter; microbial composition

check for updates

Academic Editor: Paola Grenni

Received: 31 December 2024
Revised: 4 February 2025
Accepted: 6 February 2025
Published: 10 February 2025

Citation: Pálhalmi, J.; Niemcewicz, M.; Krzowski, Ł.; Mező, A.; Szelenberger, R.; Podogrocki, M.; Bijak, M. Baseline Particulate Matter Characteristics and Microbial Composition in Air Samples from Natural and Urban Environments: A First Combined Genomic and Microscopy Analysis. *Appl. Sci.* **2025**, *15*, 1778. https://doi.org/10.3390/app15041778

Copyright: © 2025 by the authors. Licensee MDPI, Basel, Switzerland. This article is an open access article distributed under the terms and conditions of the Creative Commons Attribution (CC BY) license (https://creativecommons.org/licenses/by/4.0/).

1. Introduction

Due to climate change-driven fluctuations in airborne particulate matter (PM) content and quality, detecting airborne pathogens has become increasingly challenging for public health, pandemic preparedness, biosafety and biosecurity, food industry process monitoring, and air quality control. Several efforts have been made to establish a baseline for biological and pathogenic content in the air. However, despite advancements in standardizing general air quality monitoring based on PM ranges, there are still no definitive guidelines or standards addressing the baseline levels of bio- and pathogen content in the atmosphere [1,2].

Biomass, a critical component of ecosystems, serves as a fundamental measure of the amount of living or recently living organic material. Understanding its concentration is vital for ecological studies and also for detection purposes [3]. Notably, biomass concentration exhibits significant variability not only seasonally but also across different sampling locations. Seasonal changes profoundly affect biomass concentration due to variations in temperature, light, and moisture, which directly impact growth and the activity of other organisms. Many species reproduce during these seasons, contributing to higher biomass. The concentration of biomass also varies significantly across different sampling locations due to diverse environmental conditions, habitat types, and human activities [4–8].

One of the crucial methods for analyzing air samples involves collecting and examining particles on microscopic slides [9]. The presence of contaminants known as "background noise" in air samples hinders the analysis process due to seasonal fluctuations. "Background noise" in air samples consists of a variety of PM, that can include dust, pollen, spores, soot, and other microscopic particles. These particles are ubiquitous and can originate from natural sources like soil, plants, and water bodies, as well as human activities such as industrial processes, vehicle emissions, and construction work. These sources exhibit seasonal variability, with biological particulates experiencing a marked increase during spring and early summer in continental climates due to heightened microbial activity. Airborne PM in the 2.5–10 μm range, composed of organic compounds, dust, inorganic materials (e.g., quartz, silica, mineral oxides), and biological constituents, contributes significantly to chronic respiratory conditions. Among these, bacterial particles were specifically linked to various pulmonary diseases and chronic respiratory inflammation. However, the composition of PM varies substantially depending on local geolocation-specific activities and emission sources [7,8,10,11].

Recent advancements in DNA sequencing technology have significantly expanded the potential for the genomic analysis of air samples. This innovative approach allows us to gain a deeper understanding of the microbiological composition of the atmosphere, which is crucial for public health (pathogen detection), agriculture, and environmental protection [12]. The advancement of genomic technologies has revolutionized environmental monitoring, particularly in the analysis of airborne microorganisms. While genomic analysis allows for the precise detection and identification of pathogens and other biological particles, optical methods such as quantitative phase imaging (QPI) light microscopy offer rapid pathogen detection, particularly for bacterial-sized particles [13,14]. Extensive genomic analyses were conducted on the microbiome of air samples from closed environments and crowded public spaces [15]. However, no comparative analysis has yet been conducted to investigate the relationship between the genomic sequencing data of bacterial species and the PM characteristics of airborne particles within the bacterial size range across distinct geolocations sampled in the same season.

Understanding the variability in PM size distributions and statistical characteristics across geolocations with distinct activity profiles, combined with the genomic sequence analysis of bacterial components, is essential for establishing a baseline for airborne bio-

component and biothreat detection [16]. Such baselines are critical for informed decision-making in response to both incident-related and naturally occurring outbreaks. To explore baseline differences in PM ranges and genomic bacterial content, two geolocations with contrasting activity profiles, yet in close proximity, were selected for air sampling: an urban area near a high-traffic roadway and a natural environment within a forested region. Due to recent technical advancements and several promising efforts to develop low-cost, portable microscope prototypes, artificial intelligence-powered microscopy has emerged as a practical tool for environmental air quality monitoring [13,17,18]. Additionally, this technology has proven useful for air bacterial content detection in scenarios driven by chemical, biological, radiological and nuclear (CBRN) threats, public safety, and security needs [19,20]. However, comparative statistical data on the baseline size and shape characteristics of airborne particles remain unavailable for samples collected from nearby environmental sites with distinct activity profiles.

Biological agents, especially bacteria, are very diverse and can be characterized by their diverse structure, shapes, and sizes. In regard to the bacteria size, the average range is from 0.2 μm to 2 μm, which allows them to be visualized by optical microscopy techniques [21]. The diversity of bacteria shapes allows us to identify them within their genus and distinguish them from other bacterial genera. On the basis of bacteria shapes, they can be classified into four categories: spherical bacteria, spiral bacteria, rod-shaped bacteria, and filamentous bacteria. Besides the four main bacteria shapes, irregular shapes are also present: appendage, pleomorphic, star-shaped, sheathed, stalk, spindle-shaped, lobed, trichome-forming, or rectangular. When examining the bacteria arrangements, they may group in pairs (diplo), in groups of four (tetrads), in grape like (staphylo) formations, or in chains (strepto) [22]. These characteristics can be tabulated and can create a form of a catalogue—database.

The primary objective of this study was to assess the statistical differences in PM characteristics (including features like diameter, area, perimeter, length, and width) across two sites with contrasting human and natural activity profiles within a localized region. The secondary objective was to analyze the microbial, specifically bacterial, content of air samples from these locations.

The rapid detection and identification of biological agents, whether for medical diagnostics, environmental monitoring, or biodefense, is a critical challenge in contemporary science. The results obtained from microscopic examinations combined with genetic studies, which enable the identification of the observed biomass, form the basis for the development of advanced techniques. These, in conjunction with the rapidly developing technology of deep machine learning, will allow for the rapid detection of changes in the characteristics of PM and microbial composition, particularly within the scope of CBRN threats.

2. Materials and Methods

2.1. Air Sample Collection

Air sample collection was carried out in the spring season (April 2024). The samples were collected at two fundamentally different but close geolocations (urban area and forest region) to compare the baseline PM and microbial load of different microenvironments close to each other. The two locations were a forest/lake location and a parking/urban area with a heavy traffic road nearby, as indicated on the map segment below by number 1 (forest/lake) and 2 (urban/parking area) (Figure 1). For air sampling, the Coriolis Compact device (Bertin Technologies SAS, Montigny-le-Bretonneux, France) was used for 9 min to sample 450 L of air to comply with the NATO Handbook for Sampling and Identification of Biological, Chemical and Radiological Agents (SIBCRA)—Allied Engineering Publication (AEP) 66: the procedures and techniques in terms of the minimal and maximum recommended volume

of air (100–1000 L) under an intentional biothreat release scenario. Two samples were taken right after each other, one for microscopy, and the other for genomic analysis. The samples were dissolved in 1 mL of physiological saline. In order to calibrate the sampling procedure, the amount of 3 mL of buffer was used to wash the tube after air sampling. The samples were transported to the laboratories in suitable temperature conditions.

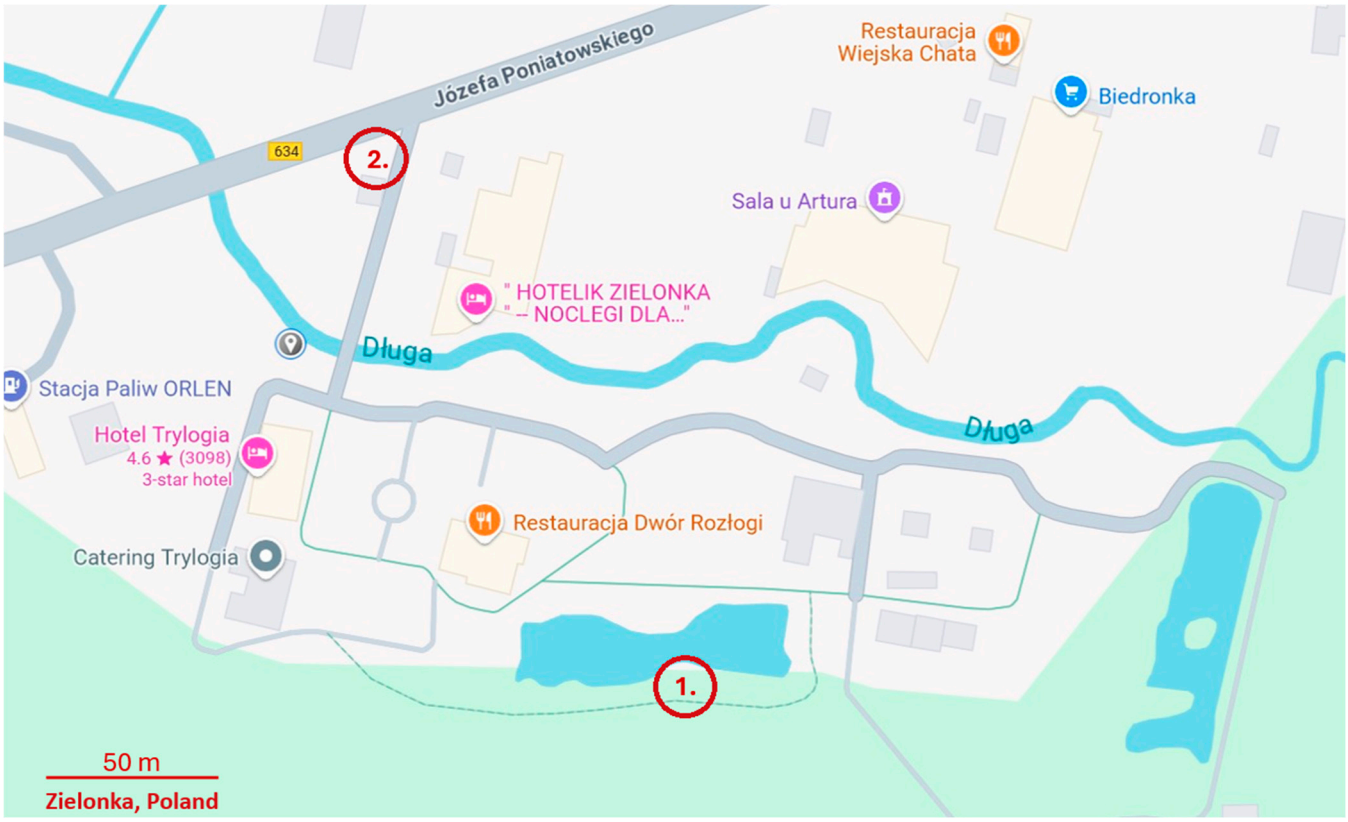


Figure 1. Map of geolocation. Forest area is indicated by 1, and urban area is indicated by 2.

2.2. Microscopic Analysis

Differential interference contrast (DIC) images (NIKON Eclipse Ti2 light microscope, Tokyo, Japan) were captured at 125 different locations. A volume of 20 µL of the dissolved, unstained air sample (collected from forest and urban areas) was placed onto a glass microscope slide and covered with a coverslip. Furthermore, the slides were allowed to rest for 5 min to stabilize the biomass in the aqueous phase. All slides were prepared using the calibration bar (10 µm), which allowed for the proper measurement of the size of the unknown object captured. In order to obtain the proper sample thickness (to avoid a large amount of biomass), 2–4 times dilution is recommended. The internal software of the microscope (NIS-Elements) was used to calculate the physical dimensional features of the particles detected: diameter, area, perimeter, length, and width. Detailed particle feature analysis was carried out on the air samples collected during the spring season. The statistical analysis of the particle features was carried out by custom-created codes in MATLAB 2024a software (MathWorks, Natick, MA, USA). To analyze the differences between the particle features sampled from the two locations (forest and urban areas) pairwise non-parametric comparisons were performed (Wilcoxon Rank-Sum Test and Two-Sample Kolmogorov–Smirnov Test). Bonferroni-corrected *p*-values were also calculated to reduce the likelihood of incorrect decision-making influenced by false positive events.

2.3. Genomic Analysis

For sequencing and analysis purposes, the protocol provided by Reska et al. with modification was used [23]. DNA was extracted from air samples collected using the Coriolis device. DNA extraction was performed using the Qiagen PowerFecal® Pro DNA Kit (QIAGEN, Hilden, Germany), following the manufacturer's protocol, with 50 µL of elution buffer for final elution. The final DNA concentration was measured with the highest precision using the Quantus™ Fluorometer (Promega, Madison, WI, USA) and the highly sensitive QuantiFluor dsDNA kit, with 1 µL of DNA eluate used per sample to ensure an accurate concentration assessment. A shotgun nanopore sequencing (with cutting-edge technology) approach was applied using the Ligation Sequencing Kit (SQK-LSK109), MinION R9.4.1 flow cells, and MinKNOW v23.04.3 software (Oxford Nanopore Technologies, Oxford, UK), enabling real-time, high-throughput sequencing of environmental DNA extracted from airborne particles.

Following DNA fragmentation and adapter ligation, the libraries were purified using AMPure XP magnetic beads (Beckman Coulter, Brea, CA, USA) to remove short DNA fragments and potential contaminants. The AMPure bead purification ensured high-quality library preparation by selectively binding DNA fragments above the threshold size, optimizing sequencing performance. For environmental sample sequencing, one R9.4.1 MinION flow cell per sample type (forest and urban areas) was utilized to ensure sufficient sequencing depth and comprehensive microbial representation.

The sequencing parameters were set with meticulous attention to detail, including a minimum read length of 200 bases, and translocation speed of 450 bases per second, with each sequencing run lasting 72 h. The MinKNOW v23.04.3 was used for the samples, and these sequencing data were generated at a signal measurement frequency of 4 kHz. For the purpose of signal converting, the Guppy v 6.5.7—bioinformatics toolkit that enables real-time basecalling in fast mode was used [24]. All collected data passed the FASTQ format and the files were analyzed via Oxford Nanopore Software EPI2ME v 3.7.3 in order for the real-time analysis of nanopore sequencing data [25]. In this study, taxonomic classification of sequencing reads was conducted using the What's In My Pot (WIMP) workflow in Oxford Nanopore's EPI2ME v3.7.3 platform [26]. WIMP is a cloud-based, automated classification tool designed for analyzing metagenomic data generated from Oxford Nanopore sequencing.

The classification of the WIMP process relies on the NCBI RefSeq database, which contains high-quality, manually curated genomic sequences from a diverse range of microbial taxa. WIMP uses Centrifuge, a high-performance taxonomic classifier, in order to compare k-mers (short DNA sequence fragments) from the sequencing reads against a reference database. All generated data were analyzed to the genus and species level, ensuring a comprehensive understanding of the obtained results.

3. Results

3.1. Microscopic Analysis

Descriptive statistical analysis was conducted as an initial step to characterize the fundamental statistical properties of the particle feature distributions, including the mean, median, standard deviation (STD), and range, as defined by the minimum (Min) and maximum (Max) values. The results of this analysis are presented in Tables 1 and 2, summarizing the particle populations sampled from the forest and urban areas, respectively.

Table 1. Descriptive statistical analysis of the particle samples collected in the forest. Feature dimensions: μm and μm^2 in the case of area.

Particle Feature	Mean	Median	STD	Max	Min
Diameter (μm)	1.7	0.99	2.53	25.27	0.36
Area (μm^2)	7.26	0.76	40.53	501.68	0.1
Perimeter (μm)	10.23	4.24	37.19	469.51	1.21
Length (μm)	4.38	1.73	18.37	232.6	0.38
Width (μm)	0.78	0.43	0.73	4.55	0.18
Number of particles	178	178	178	178	178

Table 2. Descriptive statistical analysis of the particle samples collected in the urban area. Feature dimensions: μm and μm^2 in the case of area.

Particle Feature	Mean	Median	STD	Max	Min
Diameter (μm)	1.09	0.7	1.42	15.87	0.36
Area (μm^2)	2.5	0.38	13.77	197.91	0.1
Perimeter (μm)	6.15	2.76	15.27	185.77	1.21
Length (μm)	2.61	0.96	7.46	91.62	0.38
Width (μm)	0.49	0.37	0.36	3.65	0.17
Number of particles	319	319	319	319	319

Descriptive statistical analysis of the particle features (diameter, area, perimeter, length, width) measured from the air samples collected from the two locations revealed that not only the number of particles, but also the variability of the particle features shows prominent differences. While the particle concentration detected by DIC microscopy was lower in the samples collected in the forest region (20 particles/L) compared to the urban area (35 particles/L), all the measured particle features showed a higher range and standard deviation sampled from the forest region.

The raw data for measuring particle features and comparing the two sampling locations were obtained from DIC microscope images (Figure 2).

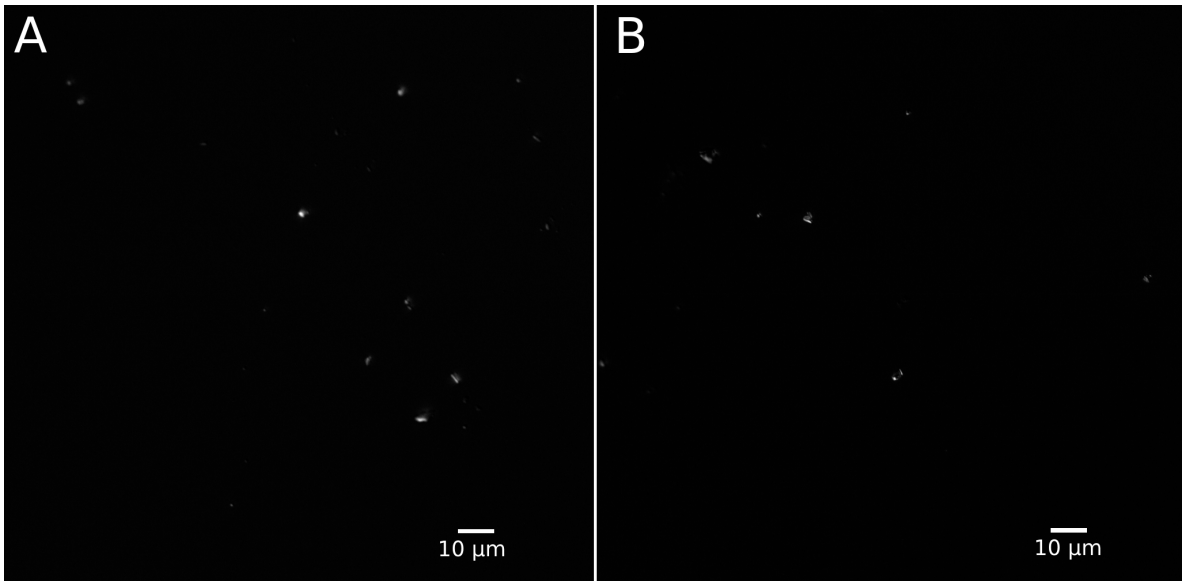


Figure 2. Representative DIC microscope images illustrate characteristics of particle populations sampled from forest (**A**) and urban (**B**) areas.

3.2. Statistical Visualization of the Particle Features Measured from the Samples Collected in the Forest and in the Urban Area

The empirical cumulative distribution function (ECDF) and Box plot representations were utilized to provide a comprehensive analysis and comparison of the particle feature distributions for the samples obtained from the forest and urban areas (Figures 3–7). The ECDF was employed to illustrate the cumulative probability distribution of the particle features, offering insights into their variability and overall distribution trends. In parallel, the Box plot representation provided a detailed summary of the key statistical parameters, including the median, interquartile range (IQR), and potential outliers, enabling a clear visualization of differences between the two sampling environments.

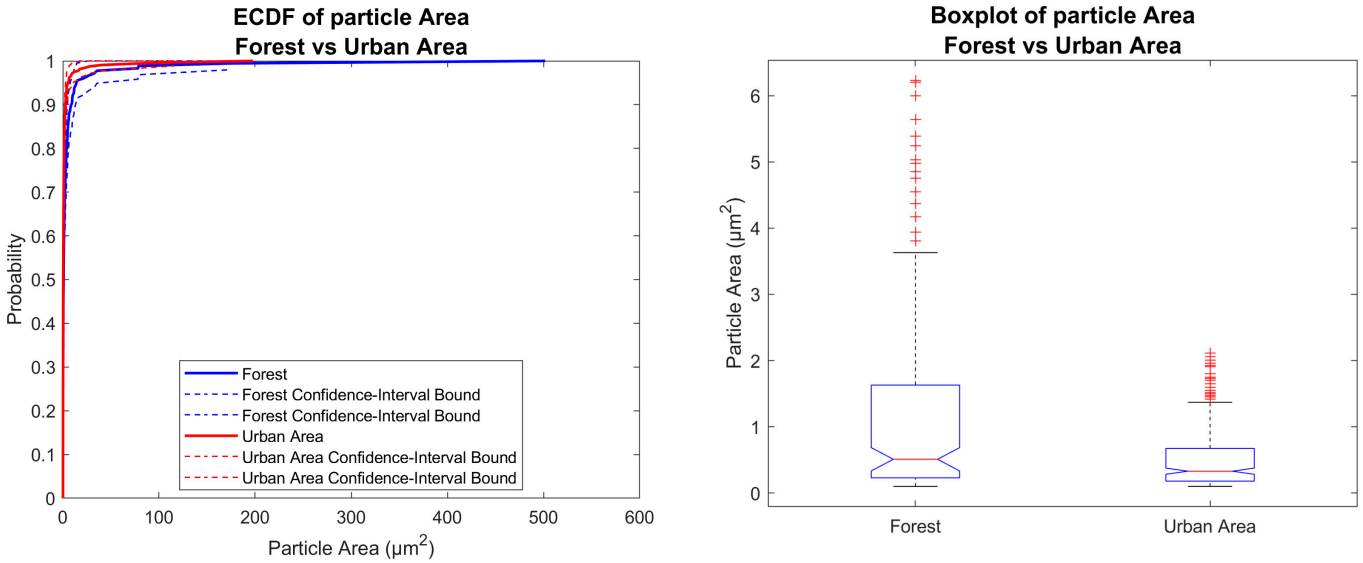


Figure 3. ECDF and Box plot representation of particle feature "Area" calculated by DIC microscopy.

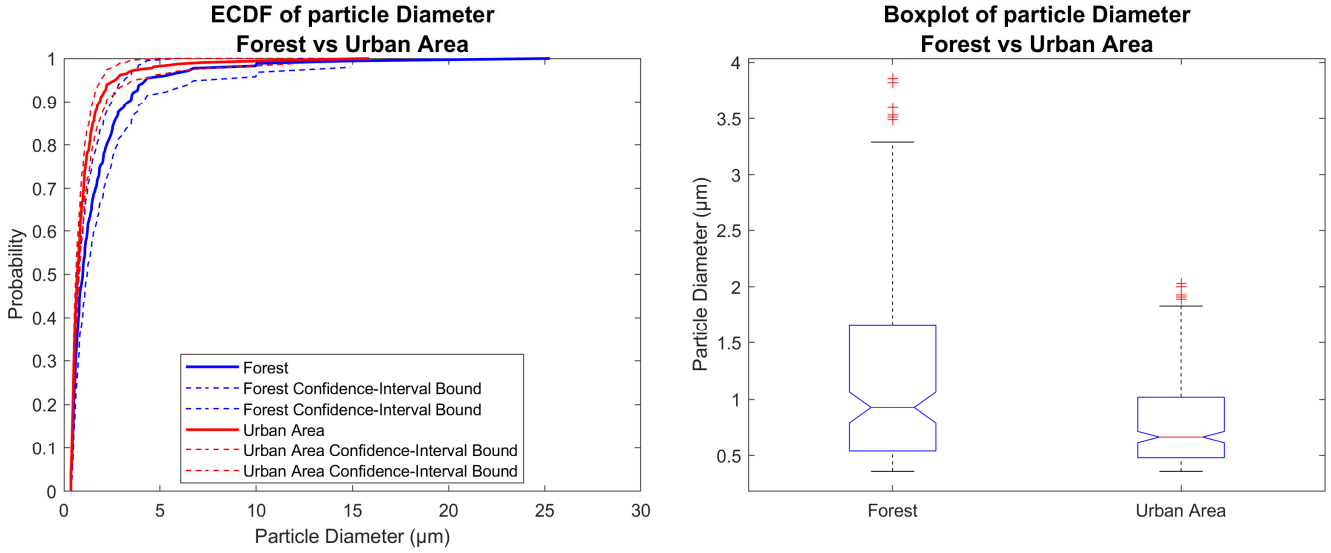


Figure 4. ECDF and Box plot representation of particle feature "Diameter" calculated by DIC microscopy.

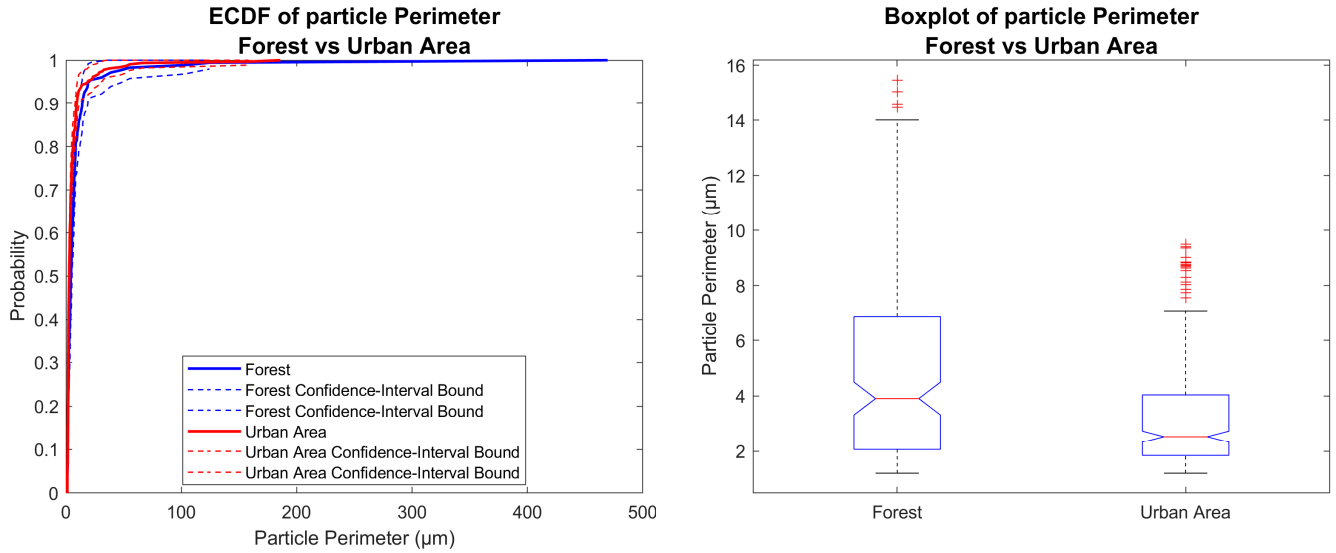


Figure 5. ECDF and Box plot representation of particle feature "Perimeter" calculated by DIC microscopy.

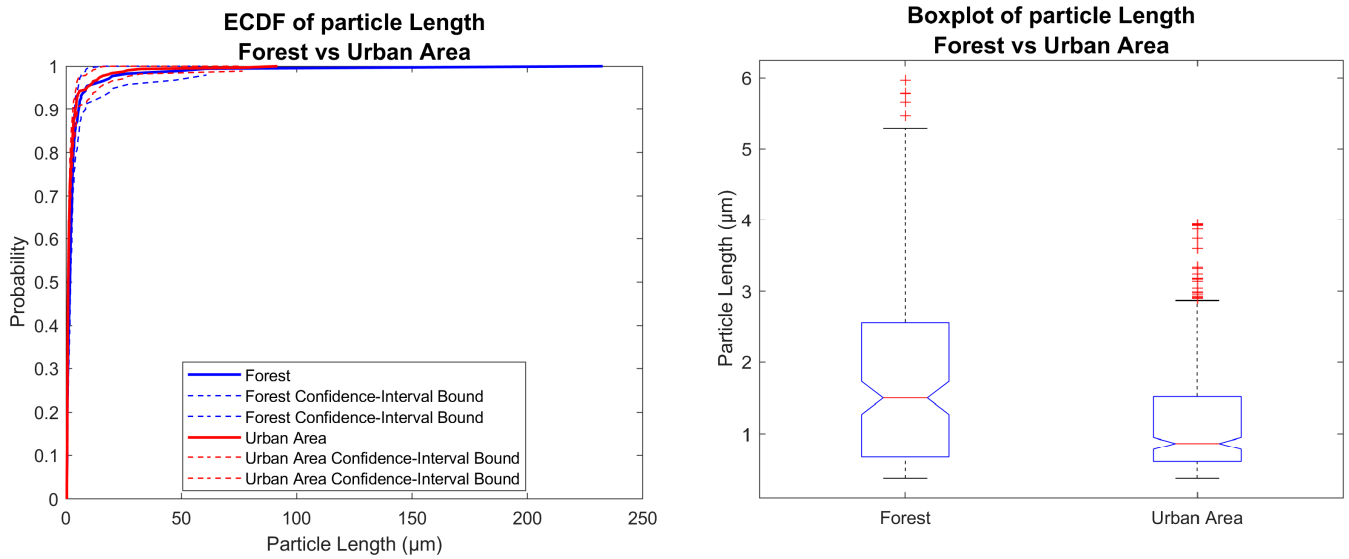


Figure 6. ECDF and Box plot representation of particle feature "Length" calculated by DIC microscopy.

Non-parametric statistical analysis of the air particle features collected in the forest and urban areas showed that the samples are distinguishable based on the sampling location in the case of all features. Two different non-parametric statistical tests were applied to determine if two independent samples come from the same distribution: Wilcoxon Rank-Sum Test, and Two-Sample Kolmogorov–Smirnov Test. The p-values and the Bonferroni-corrected p-values result from pairwise non-parametric comparisons, as presented in Table 3. According to the p-values, since $p < 0.01$ for all the compared features, we could conclude that the samples collected from the forest and urban areas show significant statistical difference. Despite a slight elevation in Bonferroni-corrected p-values (Table 3), all values remain significantly lower than the threshold of 0.01. This indicates that the distributions of the features sampled from the forest and urban areas are significantly different ($p < 0.01$). Since the non-parametric tests can show high sensitivity against statistical sample inhomogeneity, the pattern of the differences between the two distributions was further investigated. Based on the empirical cumulative distribution function (ECDF) analysis, we can conclude that

the ECDF of the particle feature "width" represents the most prominent difference among the features, especially in the range of 0.52–1.66 µm (Figure 6).

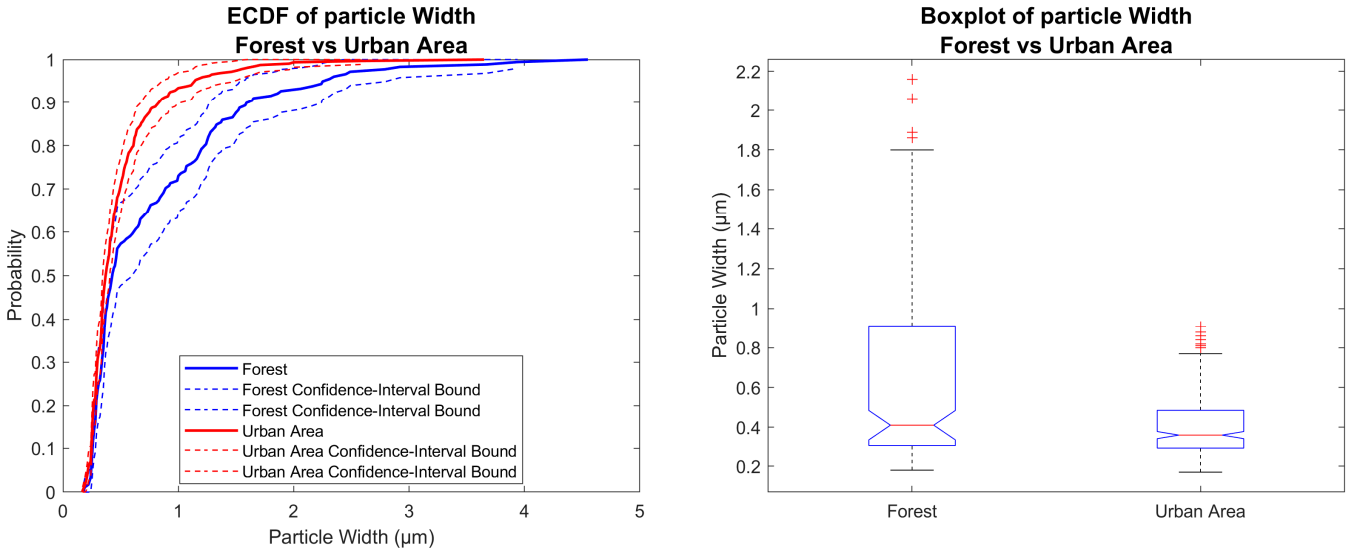


Figure 7. ECDF and Box plot representation of particle feature "Width" calculated by DIC microscopy.

Table 3. Non-parametric statistical analysis of forest and urban area samples.

Particle Features	*p*-Value; Rank-Sum	Bonferroni-Corrected, Rank-Sum	*p*-Value; KS_Test	Bonferroni-Corrected, KS_Test
Area	8.620×10^{-6}	3.448×10^{-5}	6.388×10^{-5}	2.555×10^{-4}
Diameter	2.823×10^{-6}	1.129×10^{-5}	4.146×10^{-5}	1.658×10^{-4}
Perimeter	1.897×10^{-6}	7.586×10^{-6}	5.158×10^{-6}	2.063×10^{-5}
Length	3.09×10^{-6}	1.236×10^{-5}	1.967×10^{-7}	7.868×10^{-7}
Width	7.314×10^{-6}	2.926×10^{-5}	2.976×10^{-7}	1.190×10^{-6}

Rank-Sum—Wilcoxon Rank-Sum Test; KS_Test—Two-Sample Kolmogorov–Smirnov Test.

3.3. Genomic Analysis

The sequencing analysis demonstrated significant variations in microbial community composition across the sampling sites (45 microorganisms in the forest/lake location, and 32 microorganisms in the parking/urban area). The results of sequencing the air sample collected from the parking/urban and forest/lake sites and with identification of the detected microorganisms together with their approx. sizes are presented in Tables 4 and 5. Size approximations are represented as "width × length" µm according to the data available in BioMed Big Data Center (BMDC) and BacDive [27]. Furthermore, using the Oxford Nanopore Software EPI2ME v 3.7.3 and iTOL v6 software, a dendrogram based on DNA sequencing data obtained from the air samples collected using the Coriolis air sampler was created. The dendrogram illustrates the phylogenetic relationships among microbial communities captured from different parking/urban and forest/lake sites. High-throughput sequencing and bioinformatic analyses were employed to process the environmental DNA, resulting in a comprehensive profile of airborne microorganisms. The dendrograms (Figures 6 and 7) depict the phylogenetic relationships of microorganisms identified in the forest/lake and urban locations, respectively. Each cluster represents groups of organisms with similar genetic origins, allowing for a clear identification of differences in microbial composition. The significant variations in the number and diversity of taxa between the two locations are likely influenced by environmental factors, such as pollution in the urban area and the natural biodiversity present in the forest/lake. Notable differences in microbial diversity

and abundance were observed, demonstrating the sensitivity of air sampling in detecting spatial variations in microbial communities.

Table 4. The list of microorganisms detected in the forest/lake site with their approx. sizes.

No	Microorganism	Size Approx.
1	*Escherichia*	1–1.5 × 2–6 µm
2	*Salmonella*	0.7–1.5 × 2–5 µm
3	*Shigella*	0.4–0.6 × 1–3 µm
4	*Halomonas*	0.6–0.8 × 1.6–1.9 µm
5	*Acinetobacter*	0.9–1.6 × 1.5–2.5 µm
6	*Moraxella*	1–1.5 × 1.5–2.5 µm
7	*Pseudomonas*	0.5–1.0 × 1.5–3 µm
8	*Oligotropha*	N/A
9	*Sinorhizobium*	0.8 × 2 µm
10	*Celeribacter*	0.18–1.2 × 1.2–3.4 µm
11	*Paracoccus*	0.4–0.9 × 2 µm
12	*Magnetospirillum*	0.5 × 6–7 µm
13	*Erythrobacter*	0.5–0.7 × 1–4 µm
14	*Noyosphingobium*	0.5–0.8 × 0.8–2 µm
15	*Parasphingopyxis*	N/A
16	*Sphingomonas*	0.3–0.8 × 1–2.7 µm
17	*Variovorax*	0.3–0.6 × 0.7–3 µm
18	*Janthinobacterium*	2.5 × 6 µm
19	*Massilia*	0.5–0.75 × 2.5–9.2 µm
20	*Sorangium*	0.8–1.3 × 3.7–7.7 µm
21	*Luteitalea*	0.6–0.75 × 0.9–1.4 µm
22	*Hymenobacter*	0.3 × 4 µm
23	*Aequorivita*	0.4–0.5 × 1.1–1.7 µm
24	*Flavobacterium*	0.4–0.5 × 1–5 µm
25	*Luteolibacter*	0.5–0.7 × 0.9–1.5 µm
26	*Mycobacterium*	0.2–0.6 × 1.0–10 µm
27	*Mycolicibacterium*	N/A
28	*Rhodococcus*	0.4 × 1.6 µm
29	*Geodermatophilus*	1.0–2.8 × 1.0–3 µm
30	*Brevibacterium*	0.6–1.2 × 1.5–6 µm
31	*Cellulomonas*	0.75–1.5 × 1.5–3.75 µm
32	*Brachybacterium*	0.5 × 0.5 µm
33	*Dermabacter*	0.6–0.8 × 0.9–1.1 µm
34	*Dermacoccus*	0.9 × 1.6 µm
35	*Kytococcus*	0.8 × 1.1 µm
36	*Herbiconiux*	N/A
37	*Micrococcus*	0.5 × 2 µm
38	*Isoptericola*	N/A
39	*Micromonospora*	N/A
40	*Nocardioides*	0.35 × 1.5 µm
41	*Cutibacterium*	0.4–0.7 × 3–5 µm
42	*Pseudonocardia*	N/A
43	*Streptomyces*	0.5 × 1 µm
44	*Actinomadura*	3–20 × 6–30 µm
45	*Bacillus* spp.	0.5–1.0 × 1.0–4 µm

Table 5. The list of microorganisms detected in the parking/urban site with their approx. sizes.

No	Microorganism	Size Approx.
1	*Escherichia coli*	1–1.5 × 2–6 µm
2	*Escherichia marmotae*	0.5–1 × 1–2.5 µm
3	*Salmonella enterica*	0.7–1.5 × 2–5 µm
4	*Shigella flexnerii*	0.4–0.6 × 1–3 µm
5	*Marinobacterium* sp. LSUCC0821	0.5–0.7 × 1.6–2.3 µm
6	*Acinetobacter seifertii*	1.0–1.5 × 1.5–2.5 µm
7	*Acinetobacter johnsonii*	0.9–1.6 × 1.5–2.5 µm
8	*Moraxella osloensis*	1–1.5 × 1.5–2.5 µm
9	*Pseudomona oleovorans*	0.5–1.0 × 1.5–3 µm
10	*Pseudomona denitrificans*	0.8 × 1 µm
11	*Pseudomona* sp. R32	0.5 × 0.8 µm
12	*Brevundimonas naejangsanensis*	0.4 × 2.3 µm
13	*Mesorhizobium opportunistum*	0.4–0.9 × 1.2–3 µm
14	*Rhiziobium* sp. Khangiran 2	0.5–0.9 × 1–3 µm
15	*Sinorhizobium meliloti*	0.8 × 2 µm
16	*Roseomonas* sp. FDA ARGOS_362	0.9 × 2.2 µm
17	*Sphingomonas* sp. HMP9	0.3–0.8 × 1–2.7 µm
18	*Comamonas testosteroni*	0.5 × 2 µm
19	*Hydrogenophaga* sp. BA0156	0.4–0.5 × 0.7–1.3 µm
20	*Rhodoferax saidenbachensis*	0.9 × 1.8 µm
21	*Sandaracinus amylolyticus*	0.8 × 4.5 µm
22	*Flavobacterium anhuiense*	0.3 × 1.7 µm
23	*Actinomyces oris*	0.4 × 1 µm
24	*Corynebacterium ulcerans*	0.5 × 3–5 µm
25	*Dermacoccus nishinomiyaensis*	0.9 × 1.6 µm
26	*Rhodoluna lacicola*	0.05 µm
27	*Rathayibacter* sp. VKM Ac-2759	0.5–0.7 × 1.1–2 µm
28	*Glutamicibacter arilaitensis*	N/A
29	*Cutibacterium acnes*	0.4–0.7 × 3–5 µm
30	*Aeromicrobium* sp. 592	0.5 × 1.2 µm
31	*Bacillus coagulans*	0.9 × 3–5 µm
32	*Lactococcus lactis*	0.5 × 1.5 µm

4. Discussion

This study is the first comparative analysis to quantitatively characterize baseline differences between closely situated natural and urban environments in terms of specific PM features and the combined genomic sequencing analysis of microbiome content.

The statistical analysis of particle features indicates that the two locations can be differentiated based on complex shape parameter analysis of airborne particles. In particular, particle width emerged as the most robust distinguishing feature, with statistically significant differences observed in the 0.52–1.66 µm range. This difference likely reflects a higher concentration of elongated, rod-shaped particles in one of the environments. Additionally, findings from non-quantitative genomic analysis suggest that certain bacterial strains may contribute to these particle-based quantitative differences (Tables 4 and 5).

The results demonstrate the successful identification of a broad spectrum of microbial taxa, especially bacteria (Tables 4 and 5, Figures 8 and 9). Notably, the data revealed significant differences in microbial community composition and PM feature distributions between the sampling sites (urban parking area and forest/lake site), suggesting that environmental factors may influence the detection of bioagents, which could be either intentionally or unintentionally released into the air. Furthermore, the findings highlight the potential of combining air-based environmental DNA sampling with quantitative phase imaging (QPI) microscopy as a non-invasive tool for monitoring microbial diversity.

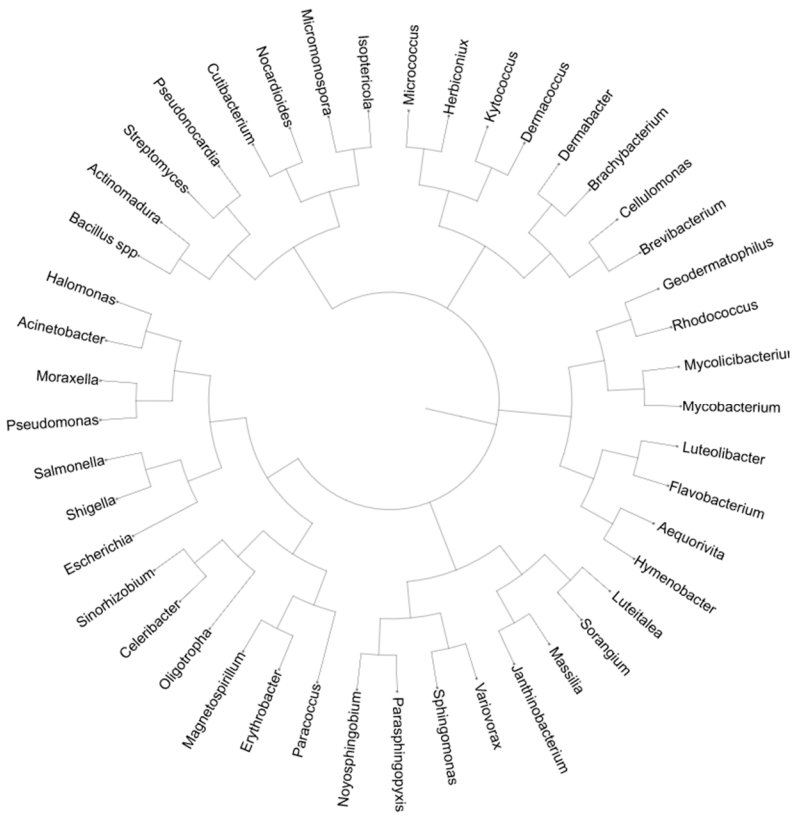


Figure 8. Phylogenetic relationships among microorganisms detected in forest/lake location. Diversity of organisms, represented by multiple unique clusters, highlights influence of this environment's biological richness.



Figure 9. Phylogenetic relationships among microorganisms detected in urban location. Fewer clusters and greater uniformity reflect limited diversity of microorganisms in urban environment.

Our results demonstrate a fundamental difference in the baseline load of air between natural and urban environments, with regard to the variability in particle features and the diversity of microbial content. Air samples from the natural environment exhibited greater variability and range in particle size, feature distribution, and a broader diversity of microbiological entities compared to the urban samples. In contrast, the air samples from the urban environment contained a higher concentration of particles, which is consistent with the presence of pollution sources. These findings are consistent with our earlier observations: biomass concentration in the air samples varies both seasonally and geographically. Specifically, total bacterial concentrations ranged from 35 CFU/m^3 in autumn to 2890 CFU/m^3 in summer, while total fungal concentrations ranged from 191 CFU/m^3 in autumn to 3237 CFU/m^3 in summer [7].

Our results, in conjunction with recent advancements in computational microscopy [19,20], support the integration of field-deployable microscopy combined with genomic identification tools into environmental air sample analysis protocols. This approach can enhance early-stage decision-making in air-based biothreat monitoring.

Our findings suggest that the ranges of particle size variability measured by DIC microscopy and calculated based on the genomic sequencing results correspond with each other, thus highlighting the importance of field-implemented protocols that integrate early-warning optical sensing methods for anomaly detection, followed by genomic analysis for verification and identification. Such an approach can be a critical framework for CBRN or public safety and security research and intervention.

The analysis and detailed identification of environmental samples obtained from air across various geolocations, considering seasonality, would enable the creation of a unique library that could facilitate the assessment of potentially hazardous changes in the current biomass. The results obtained from studies focusing on monitoring the characteristics of particulate matter and microbial compositions from different geolocations demonstrate significant importance for future perspectives, especially in the environmental monitoring area [1,28] so as to understand the baseline pattern of the airborne microbiome to support decision-making under CBRN, biosecurity, and BioDefense scenarios. This approach will enable the first responders to compare their findings with a vast array of reference material and metadata, fostering collaboration and accelerating the pace of discovery. By providing standardized protocols for combined air sample analysis, we can ensure consistency and reliability across different studies. This standardization approach is essential for reproducibility in field detection, enabling technicians to confidently build on each other's work and verify results.

In addition to applications in public safety, security, and CBRN-related scenarios, our study significantly contributes to advancing research and development in public health. By utilizing the standardized and comprehensive methodology we introduced, researchers can better understand the complex effects of particulate matter (PM) size ranges on human physiology and disease progression. This framework paves the way for more accurate and reproducible investigations, ultimately supporting the development of targeted interventions and policies to mitigate health risks associated with air pollution.

Fine particulate matter (PM2.5), with a diameter of 2.5 micrometres or less, is among the most hazardous air pollutants to human health. Its small size allows deep penetration into the alveolar regions of the lungs and potential entry into the bloodstream [29]. PM2.5 exposure is linked to inflammatory and oxidative damage, increased plaque formation in blood vessels, and the disruption of the autonomous nervous system, impacting cardiovascular health [30] and inducing acute changes even in ventricular repolarization, as indicated by QT interval alterations [31]. Globally, PM2.5 ranks as the sixth largest contributor to disease burden, with an estimated 4.7 million deaths in 2015 attributed to its exposure. It

contributes to 30% of global stroke risk and increases susceptibility to respiratory infections from various pathogens [32–35]. Studies reveal robust associations between fine particulate levels and elevated risks of lung cancer and heart attack [36].

Smaller particles, such as PM0.1, exhibit an even stronger correlation with cardiovascular dysfunction and mortality, including increased ischemic and thrombotic stroke risk and impaired microvascular function, compared to PM2.5 or PM10 [37,38]. The complex composition of PM2.5 (organic, inorganic, and microbial) and PM0.1 complicates efforts to isolate its most harmful effects on health.

Uncovering the dimensional and microbial characteristics of air through combined studies can deepen our understanding of measurement-based intervention protocols, bridging overlapping sectors such as public safety, security, public health, and CBRN.

5. Conclusions

This study aimed to compare natural and urban environments by analyzing PM characteristics and microbial diversity using QPI microscopy and genomic sequencing. The results revealed significant differences in particle morphology, microbial composition, and PM distribution between the sites, highlighting the potential of integrated optical and genomic analysis. Focusing on the detection of anomalies within specific size ranges and PM features of unstained air samples using DIC microscopy can serve as an effective early-warning detection tool in the field, prior to the accurate genomic identification of biological agents. The use of microscopy and the size parameters obtained through it will enable the rapid identification of changes occurring in the studied area, as the intentional or unintentional release of a biological agent into the air will significantly alter the composition of the collected sample, resulting in the creation of a markedly monomorphic sample. This approach is particularly useful for identifying bioagents in biothreat scenarios, which are characterized by distinct shapes and sizes. Examples include *Bacillus anthracis* spores (rod-like, approximately 1–1.5 μm), *Francisella tularensis* (coccoid-rod, 0.2–0.5 μm × 0.7–1.0 μm), *Yersinia pestis* (rod-ovoid, 0.5–0.8 × 1–3 μm), and *Clostridium botulinum* (rods, 4–6 × 0.9–1.2 μm with oval, subterminal spores) [27]. The complex, geolocation-specific statistical database developed in this study can aid in optimizing the performance of microbial content detection algorithms. It provides guidelines for setting appropriate statistical thresholds in feature space engineering, which is essential for training and fine-tuning artificial intelligence-supported computational methodologies designed for airborne biothreat detection. This represents a critical step toward establishing interoperable detection limits and thresholds for anomaly detection, advancing air quality monitoring protocols, and enhancing biosecurity, biosafety, and public health vigilance related to airborne content.

Author Contributions: Conceptualization, J.P., M.N. and M.B.; methodology, J.P., A.M. and Ł.K.; investigation, J.P., M.N. and R.S.; writing—original draft preparation, J.P., M.N. and Ł.K.; writing—review and editing, R.S. and M.P.; visualization, J.P. and Ł.K.; supervision, J.P. and M.B.; project administration, M.N.; funding acquisition, M.N. and M.B. All authors have read and agreed to the published version of the manuscript.

Funding: This research was funded by the European Union's Horizon 2020 programme, grant number 101021723.

Institutional Review Board Statement: Not applicable.

Informed Consent Statement: Not applicable.

Data Availability Statement: The original contributions presented in this study are included in the article. Further inquiries can be directed to the corresponding author.

Acknowledgments: We gratefully acknowledge Pál Vági (HUN REN Institute of Experimental Medicine) for his valuable support and consultation regarding the DIC microscope measurements.

Conflicts of Interest: Authors János Pálhalmi and Anna Mező were employed by the company DataSenseLabs Ltd. The remaining authors declare that the research was conducted in the absence of any commercial or financial relationships that could be construed as a potential conflict of interest.

References

1. Zhao, J.; Jin, L.; Wu, D.; Xie, J.W.; Li, J.; Fu, X.W.; Cong, Z.Y.; Fu, P.Q.; Zhang, Y.; Luo, X.S.; et al. Global airborne bacterial community-interactions with Earth's microbiomes and anthropogenic activities. *Proc. Natl. Acad. Sci. USA* **2022**, *119*, e2204465119. [CrossRef] [PubMed]
2. WHO. WHO Global Air Quality Guidelines. Particulate Matter (PM2.5 and PM10), Ozone, Nitrogen Dioxide, Sulfur Dioxide and Carbon Monoxide. Available online: https://www.who.int/publications/i/item/9789240034228 (accessed on 22 September 2021).
3. Nisha, P.; John, N.; Rubeena, K.A.; Thangavel, M. Biomass from Terrestrial Environments. In *Handbook of Biomass*; Thomas, S., Hosur, M., Pasquini, D., Jose Chirayil, C., Eds.; Springer Nature: Singapore, 2024; pp. 55–81.
4. Paar, M.; Berthold, M.; Schumann, R.; Dahlke, S.; Blindow, I. Seasonal Variation in Biomass and Production of the Macrophyto-benthos in two Lagoons in the Southern Baltic Sea. *Front. Earth Sci.* **2021**, *8*, 542391. [CrossRef]
5. Arndal, M.F.; Illeris, L.; Michelsen, A.; Albert, K.; Tamstorf, M.; Hansen, B.U. Seasonal Variation in Gross Ecosystem Production, Plant Biomass, and Carbon and Nitrogen Pools in Five High Arctic Vegetation Types. *Arct. Antarct. Alp. Res.* **2009**, *41*, 164–173. [CrossRef]
6. Heid, L.; Calvaruso, C.; Andrianantenaina, A.; Granier, A.; Conil, S.; Rathgeber, C.B.K.; Turpault, M.-P.; Longdoz, B. Seasonal time-course of the above ground biomass production efficiency in beech trees (*Fagus sylvatica* L.). *Ann. For. Sci.* **2018**, *75*, 31. [CrossRef]
7. Chmiel, M.; Kral, I.; Lenart-Boroń, A. Concentration and size distribution of microbial aerosol in the historical objects in Kraków as a potential health risk and biodeterioration factor. *Aerobiologia* **2019**, *35*, 743–758. [CrossRef]
8. Liu, H.; Zhang, X.; Zhang, H.; Yao, X.; Zhou, M.; Wang, J.; He, Z.; Zhang, H.; Lou, L.; Mao, W.; et al. Effect of air pollution on the total bacteria and pathogenic bacteria in different sizes of particulate matter. *Environ. Pollut.* **2018**, *233*, 483–493. [CrossRef]
9. Azari, A.; Vanoirbeek, J.A.J.; Van Belleghem, F.; Vleeschouwers, B.; Hoet, P.H.M.; Ghosh, M. Sampling strategies and analytical techniques for assessment of airborne micro and nano plastics. *Environ. Int.* **2023**, *174*, 107885. [CrossRef] [PubMed]
10. Wang, Q.; Liu, S. The Effects and Pathogenesis of PM2.5 and Its Components on Chronic Obstructive Pulmonary Disease. *Int. J. Chronic Obstr. Pulm. Dis.* **2023**, *18*, 493–506. [CrossRef] [PubMed]
11. Yang, J.; Kim, E.K.; Park, H.J.; McDowell, A.; Kim, Y.K. The impact of bacteria-derived ultrafine dust particles on pulmonary diseases. *Exp. Mol. Med.* **2020**, *52*, 338–347. [CrossRef]
12. Sajjad, B.; Hussain, S.; Rasool, K.; Hassan, M.; Almomani, F. Comprehensive insights into advances in ambient bioaerosols sampling, analysis and factors influencing bioaerosols composition. *Environ. Pollut.* **2023**, *336*, 122473. [CrossRef]
13. Kim, G.; Ahn, D.; Kang, M.; Park, J.; Ryu, D.; Jo, Y.; Song, J.; Ryu, J.S.; Choi, G.; Chung, H.J.; et al. Rapid species identification of pathogenic bacteria from a minute quantity exploiting three-dimensional quantitative phase imaging and artificial neural network. *Light Sci. Appl.* **2022**, *11*, 190. [CrossRef] [PubMed]
14. Molani, A.; Pennati, F.; Aliverti, A.; Pálhalmi, J. Properties and Perspectives of Digital Holographic Microscopy for Bioaerosol Detection. In Proceedings of the 2023 IEEE International Conference on Metrology for eXtended Reality, Artificial Intelligence and Neural Engineering (MetroXRAINE), Ancona, Italy, 25–27 October 2023; pp. 735–740.
15. Zhao, Y.; Mao, K.; Cao, H.; Wang, B.; Zheng, X.; Du, W.; Zhang, X.; Zhang, H. Nonnegligible pathogenic exposure risk of coarse part of PM10 in non-open environments. *Front. Environ. Sci.* **2022**, *10*, 1006209. [CrossRef]
16. Bowers, R.M.; McLetchie, S.; Knight, R.; Fierer, N. Spatial variability in airborne bacterial communities across land-use types and their relationship to the bacterial communities of potential source environments. *ISME J.* **2011**, *5*, 601–612. [CrossRef] [PubMed]
17. Wu, Y.-C.; Shiledar, A.; Li, Y.-C.; Wong, J.; Feng, S.; Chen, X.; Chen, C.; Jin, K.; Janamian, S.; Yang, Z.; et al. Air quality monitoring using mobile microscopy and machine learning. *Light Sci. Appl.* **2017**, *6*, e17046. [CrossRef]
18. Paquin, P.; Durmort, C.; Paulus, C.; Vernet, T.; Marcoux, P.R.; Morales, S. Spatio-temporal based deep learning for rapid detection and identification of bacterial colonies through lens-free microscopy time-lapses. *PLoS Digit. Health* **2022**, *1*, e0000122. [CrossRef]
19. Pálhalmi, J.; Mező, A. AI-Powered Microscopy Platform for Airborne Biothreat Detection. In *Paradigms on Technology Development for Security Practitioners*; Gkotsis, I., Kavallieros, D., Stoianov, N., Vrochidis, S., Diagourtas, D., Akhgar, B., Eds.; Springer Nature Switzerland: Cham, Switzerland, 2025; pp. 117–127. [CrossRef]
20. Molani, A.; Mihalik, B.; Pennati, F.; Rahi, P.; Mező, A.; Pálhalmi, J.; Aliverti, A.; Bela, G. Advancing early detection of biological events by digital holographic microscopy and simulation of microorganisms. *Eur. Phys. J. Plus* **2024**, *139*, 879. [CrossRef]

21. Levin, P.A.; Angert, E.R. Small but Mighty: Cell Size and Bacteria. *Cold Spring Harb. Perspect. Biol.* **2015**, *7*, a019216. [CrossRef] [PubMed]
22. Young, K.D. The selective value of bacterial shape. *Microbiol. Mol. Biol. Rev.* **2006**, *70*, 660–703. [CrossRef] [PubMed]
23. Reska, T.; Pozdniakova, S.; Borràs, S.; Perlas, A.; Sauerborn, E.; Cañas, L.; Schloter, M.; Rodó, X.; Wang, Y.; Winkler, B.; et al. Air monitoring by nanopore sequencing. *ISME Commun.* **2024**, *4*, ycae099. [CrossRef] [PubMed]
24. Guppy Protocol—Oxford Nanopore Technologies. Available online: https://nanoporetech.com/document/Guppy-protocol (accessed on 4 February 2025).
25. EPI2ME Platform—Oxford Nanopore Technologies. Available online: https://nanoporetech.com/document/epi2me (accessed on 4 February 2025).
26. EPI2ME WIMP Workflow: Quantitative, Real-Time Species Identification from Metagenomic Samples—Oxford Nanopore Technologies. Available online: https://nanoporetech.com/resource-centre/epi2me-wimp-workflow-quantitative-real-time-species-identification-metagenomic (accessed on 4 February 2025).
27. Reimer, L.C.; Sardà Carbasse, J.; Koblitz, J.; Ebeling, C.; Podstawka, A.; Overmann, J. BacDive in 2022: The knowledge base for standardized bacterial and archaeal data. *Nucleic Acids Res.* **2022**, *50*, D741–D746. [CrossRef]
28. Cáliz, J.; Triadó-Margarit, X.; Camarero, L.; Casamayor, E.O. A long-term survey unveils strong seasonal patterns in the airborne microbiome coupled to general and regional atmospheric circulations. *Proc. Natl. Acad. Sci. USA* **2018**, *115*, 12229–12234. [CrossRef]
29. Shi, Y.; Ji, Y.; Sun, H.; Hui, F.; Hu, J.; Wu, Y.; Fang, J.; Lin, H.; Wang, J.; Duan, H.; et al. Nanoscale characterization of PM2.5 airborne pollutants reveals high adhesiveness and aggregation capability of soot particles. *Sci. Rep.* **2015**, *5*, 11232. [CrossRef] [PubMed]
30. Marshall, J. PM 2.5. *Proc. Natl. Acad. Sci. USA* **2013**, *110*, 8756. [CrossRef] [PubMed]
31. Peralta, A.A.; Schwartz, J.; Gold, D.R.; Coull, B.; Koutrakis, P. Associations between PM(2.5) metal components and QT interval length in the Normative Aging Study. *Environ. Res.* **2021**, *195*, 110827. [CrossRef]
32. Li, B.; Ma, Y.; Zhou, Y.; Chai, E. Research progress of different components of PM2.5 and ischemic stroke. *Sci. Rep.* **2023**, *13*, 15965. [CrossRef] [PubMed]
33. Yang, L.; Li, C.; Tang, X. The Impact of PM2.5 on the Host Defense of Respiratory System. *Front. Cell Dev. Biol.* **2020**, *8*, 91. [CrossRef]
34. Forouzanfar, M.H.; Afshin, A.; Alexander, L.T.; Anderson, H.R.; Bhutta, Z.A.; Biryukov, S.; Brauer, M.; Burnett, R.; Cercy, K.; Charlson, F.J.; et al. Global, regional, and national comparative risk assessment of 79 behavioural, environmental and occupational, and metabolic risks or clusters of risks, 1990–2015: A systematic analysis for the Global Burden of Disease Study 2015. *Lancet* **2016**, *388*, 1659–1724. [CrossRef]
35. Griffin Dale, W. Atmospheric Movement of Microorganisms in Clouds of Desert Dust and Implications for Human Health. *Clin. Microbiol. Rev.* **2007**, *20*, 459–477. [CrossRef] [PubMed]
36. Dockery, D.W.; Pope, C.A., 3rd; Xu, X.; Spengler, J.D.; Ware, J.H.; Fay, M.E.; Ferris, B.G., Jr.; Speizer, F.E. An association between air pollution and mortality in six U.S. cities. *N. Engl. J. Med.* **1993**, *329*, 1753–1759. [CrossRef]
37. Marris, C.R.; Kompella, S.N.; Miller, M.R.; Incardona, J.P.; Brette, F.; Hancox, J.C.; Sørhus, E.; Shiels, H.A. Polyaromatic hydrocarbons in pollution: A heart-breaking matter. *J. Physiol.* **2020**, *598*, 227–247. [CrossRef]
38. Izzotti, A.; Spatera, P.; Khalid, Z.; Pulliero, A. Importance of Punctual Monitoring to Evaluate the Health Effects of Airborne Particulate Matter. *Int. J. Environ. Res. Public Health* **2022**, *19*, 10587. [CrossRef] [PubMed]

Disclaimer/Publisher's Note: The statements, opinions and data contained in all publications are solely those of the individual author(s) and contributor(s) and not of MDPI and/or the editor(s). MDPI and/or the editor(s) disclaim responsibility for any injury to people or property resulting from any ideas, methods, instructions or products referred to in the content.